DOI: 10.1002/chem.200600792

Carbon Dioxide Activation by Surface Excess Electrons: An EPR Study of the CO_2^- Radical Ion Adsorbed on the Surface of MgO

Mario Chiesa* and Elio Giamello[a]

Abstract: The CO_2^- radical anion has been generated at the surface of MgO by direct electron transfer from surface trapped excess electrons and characterized by electron paramagnetic resonance spectroscopy. Both ^{13}C and ^{17}O hyperfine structures have been resolved for the first time, leading to a detailed mapping of the unpaired electron spin density distribution over the entire radical anion. The magnetic equivalence of the two O nuclei has been ascertained allowing a side-on adsorption structure at low-coordinate Mg^{2+} ions to be proposed for the surface stabilized radical.

Keywords: CO_2 activation · electron transfer · EPR spectroscopy · MgO surface

Introduction

One of the imposing challenges of contemporary chemistry is the search for new reaction pathways that may lead to the conversion of potentially noxious compounds into useful products. A relevant example in this context and a challenge in "green chemistry", is the conversion of CO_2 into fine chemicals.

Carbon dioxide is one of the most common greenhouse gases in the atmosphere but also represents a cheap and available source of C_1. It is a totally renewable feedstock compared to oil or coal and its use in the synthesis of organic compounds could have a significant positive impact on the global carbon balance.[1,2] However the exploitation of this molecule is seriously hampered by its thermodynamic stability and its rather high kinetic activation, thus a relevant external supply of thermal, electrical, or radiation energy is needed for its activation. In this context, there have been a number of investigations dealing with the activation of CO_2 either by classical coordination chemistry with transition metals[3,4] or transition metal complexes,[5] or by electron transfer from solid surfaces in typical heterogeneous catalytic processes.[6–9]

[a] Dr. M. Chiesa, Prof. E. Giamello
Dept. Chimica IFM and NIS Centre of Excellence
Università di Torino
Via P. Giuria, 7, 10125-Torino (Italy)
Fax: (+39) 011-6707855
E-mail: m.chiesa@unito.it

The reduction of CO_2 to the radical anion CO_2^- represents thus an important mode of activation. The electron affinity of CO_2 has been experimentally determined[10] to be -0.6 eV by collisional ionization experiments with alkali metals. Despite its negative electron affinity, the CO_2^- radical anion is relatively stable as a consequence of the barrier due to the change in molecular geometry. CO_2 contains, in fact, 16 valence electrons that are accommodated in the molecular bonding orbitals. When the extra electron is introduced to form the 17-electron CO_2^- radical anion, the 17th electron will occupy, according to the scheme presented by Walsh,[11] an orbital ($4a_1$) built from both s and p orbitals on the carbon atom, which will force the molecule to bend (see Figure 1).

The vibrational spectrum of CO_2^- was obtained in a neon matrix;[12] however, the deepest insights into the nature of this radical species come from electron paramagnetic resonance (EPR) spectroscopy. The first observation of this radical was reported in alkali halide matrices by γ irradiation of sodium formate,[13] and further substantiated by Ovenall and Whiffen[14] whose analysis of the data from EPR measurements showed them to be consistent with expectation, yielding a bond angle of 134°, which is identical with that for the isoelectronic NO_2.

The CO_2^- radical has also been formed on a rotating cryostat by alternatively depositing Na or K and CO_2 at low temperature,[15,16] while the Li^+–CO_2^- complex has been generated by simultaneously condensing the metallic vapor and gaseous CO_2 on a cold target. From the EPR spectrum a valence bond angle of 130° was calculated for this last spe-

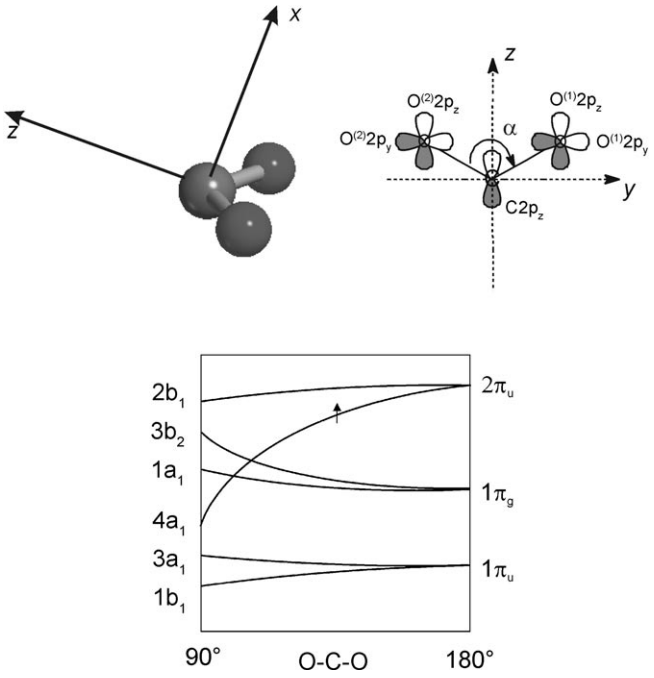

Figure 1. Reference axis system and definition of the atomic p orbitals adopted in the text, and Walsh diagram of CO_2 orbital energies in linear and bent geometries.

cies in agreement with estimates obtained from vibrational spectroscopy.[17]

Relevant to heterogeneous catalysis is however the formation and characterization of the CO_2^- radical anion at solid surfaces. For metal surfaces, considerable literature exists on the CO_2 surface chemistry, which is covered by two comprehensive review articles,[6,18] and oxides are receiving increasing attention from the surface science community.[19]

In the quest for a CO_2 reduction system that operates under mild conditions, photocatalytic reduction of carbon dioxide over semiconducting and insulating oxides in the presence of gas-phase reductants (H_2O, H_2, CH_4) is an appealing process. Since the first reports by Inoue et al.,[20] and by Gratzel and co-workers,[21] which described the photoelectrocatalytic reduction of carbon dioxide in aqueous suspensions of semiconductor powders and the methanation and photo-methanation of CO_2 over TiO_2 under mild conditions, respectively, many other similar reports have followed.[22–24] Common to all these processes is the formation of the surface-stabilized CO_2^- radical;[25] however, a thorough characterization of this important intermediate on oxide surfaces is still lacking. In particular no EPR data on ^{17}O-containing CO_2^- are available to verify the distribution of the spin density on the oxygen atoms, and to clarify the structure of the adsorbed radical on oxide surfaces. The scope of the present work is thus to provide a detailed EPR characterization of the surface-stabilized carboxylate radical anion generated by direct electron transfer from "electron-rich" surfaces. An alternative way of producing the CO_2^- radical anion on oxide surfaces is, in fact, through reaction of CO_2 with surface excess electrons. In this way Lunsford and Jane[26] first observed the surface-stabilized CO_2^- radical upon adsorption of CO_2 on UV-irradiated MgO containing surface trapped electrons.

The activity of our research group has been focused in the past on the investigation of electron trapping at the surface of polycrystalline insulating oxides (and in particular of alkaline-earth oxides with a NaCl structure such as MgO and CaO).[27,28] In particular, we found that morphological features such as steps, corners, or reverse corners are able to promote the dissociation of H atoms by stabilizing the two fragments (H^+ and e^-) in the form of a surface hydroxyl unit and of an excess electron, which can be described in terms of an unusual—the simplest—ion pair: $(H^+)(e^-)$. The surface of MgO decorated by electron–proton pairs acquires then an extraordinary chemical reactivity, which leads to the reduction, by electron transfer, of gaseous molecules to the corresponding radical anion. A relevant example of this reactivity is the reduction of the nitrogen molecule to form the surface-stabilized N_2^- radical, which was reported by our group.[29] The electron-rich MgO surface thus represents an ideal model system to investigate the nature of the surface-adsorbed CO_2^- radical formed by surface-to-adsorbate direct electron transfer. In an attempt to learn more about the details of formation of the CO_2^- radical and to provide an in depth characterization of this important intermediate, we provide the EPR analysis of CO_2^- formed when $^{12}CO_2$, $^{13}CO_2$, and $C^{17}O_2$ are contacted with $(H^+)(e^-)$ centers. In this way, a complete mapping of the unpaired electron spin density over the entire radical is obtained for the first time, as well as relevant structural information on the geometry of adsorption.

Results and Discussion

The ^{13}C coupling: The adsorbed CO_2^- was generated on the MgO surface by reacting the $(H^+)(e^-)$ centers with a small amount of $^{13}CO_2$ ($\approx$0.5 mbar) at room temperature. The typical axial spectral pattern due to surface $(H^+)(e^-)$ pairs[27] (Figure 2a) drops in intensity, while a new set of lines separated by about 20 mT, appears in the wings of the spectrum (Figure 2b). After a second dose of CO_2 (Figure 2c), the EPR spectrum of the excess electron centers completely vanishes and is substituted by a new signal due to the $^{12}CO_2^-$ radical (^{12}C, $I=0$), whereas the two side groups are attributed to $^{13}CO_2^-$ (^{13}C, $I=1/2$) species. The relative EPR intensities, measured by double integration, are in agreement with the relative abundance of the corresponding isotopes.

The $^{13}CO_2^-$ radical is characterized by an orthorhombic EPR spectrum that is accounted for by the spin Hamiltonian given in Equation (1),

$$\boldsymbol{H} = \beta_e \boldsymbol{BgS}/\hbar + \boldsymbol{SAI} \quad (1)$$

with $g_{yy} \ll g_{zz} < g_{xx}$ and $A_{zz} > A_{xx}, A_{yy}$. The reference axis system is shown in Figure 1 and was chosen in accord with

single crystal data relative to CO_2^- radicals trapped in sodium formate.[14] The x axis is perpendicular to the plane of the molecule, and the z axis bisects the O-C-O bond angle.

Table 1. Spin Hamiltonian parameters for the CO_2^- radical stabilized on the surface of MgO.

		g tensor			A tensor (^{13}C) [MHz]			A tensor (^{17}O) [MHz]		
	% ab	g_{xx}	g_{yy}	g_{zz}	$\lvert A_{xx}\rvert$	$\lvert A_{yy}\rvert$	$\lvert A_{zz}\rvert$	$\lvert A'_{xx}\rvert$	$\lvert A'_{yy}\rvert$	$\lvert A'_{zz}\rvert$
CO_2^- a	70				507.5	495.2	629.3	67.2	71.5	169.4
CO_2^- b	20	2.0026	1.9965	2.0009	537.6	518.9	655.9	81.0	84.1	159.7
CO_2^- c	10				unresolved			78.2	81.3	148.4

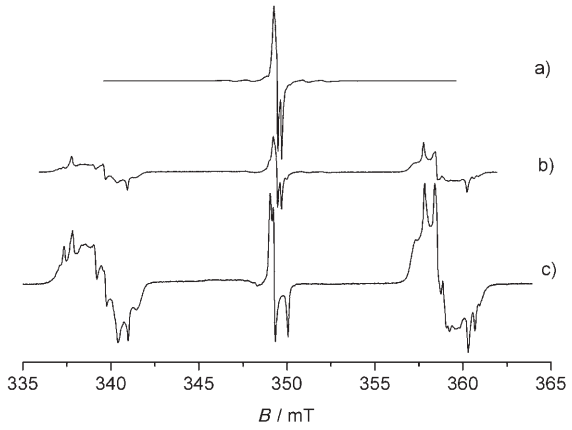

Figure 2. EPR spectra of a) (H+)(e−) centers at the surface of MgO, b) after reaction with 0.5 mbar of CO_2, c) after reaction with a second dose (0.5 mbar) of CO_2. Spectra recorded at 1 mW microwave power and 77 K.

Inspection of Figure 2b and 2c reveals that, following the first dose of CO_2, a second species is formed with slightly different spin-Hamiltonian parameters. Computer simulation of the experimental spectrum (Figure 3), based on the above Hamiltonian, allows the spin Hamiltonian parameters of the two resolved species to be identified (Table 1). A third species is probably buried within the spectral line width; however, due to the poor resolution we did not insert it in the simulation of the spectrum.

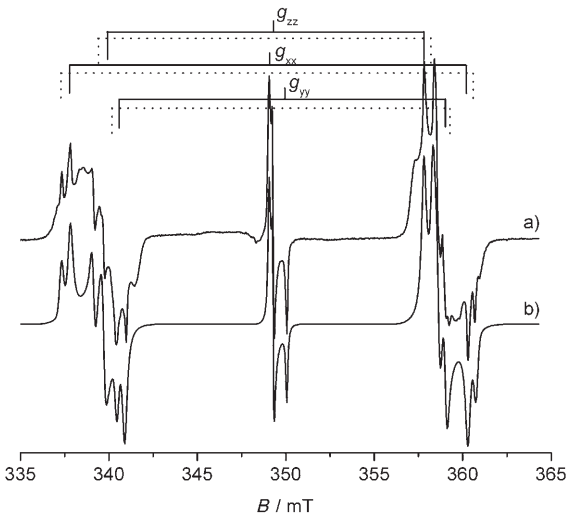

Figure 3. Experimental a) and simulated b) EPR spectrum of surface adsorbed CO_2^- radicals.

The $\boldsymbol{g}$ values of the two species are identical, within the spectral resolution, and in substantial agreement with those reported by Lunsford and Jane,[26] for the same species and in accord with data coming from CO_2^- radicals trapped in solid matrixes.[14] An educational discussion for the interpretation of the $\boldsymbol{g}$ matrix for this radical can be found in reference [30]. Here we limit ourselves to the observation that the largest deviation from the free electron g value ($g_e = 2.0023$) is expected along the y axis (g_y), and is due primarily to admixture of the ground state ($4a_1$) with the first excited state ($2b_1$), while the direction of the maximum hyperfine coupling coincides with the principal g value oriented along the z axis.

At variance with previous work,[26] the ^{13}C hyperfine matrix is, for the first time, fully resolved for both species, allowing a detailed analysis of the spin density repartition on the radical anion. The experimental hyperfine matrix reported in Table 1 can be decomposed in the usual way into the isotropic (a_{iso}) and dipolar contributions [Eq. (2)].

$$\boldsymbol{A} = a_{iso}1 + \boldsymbol{T} \tag{2}$$

This can be done if we assume, following single-crystal measurements, that all the matrix elements have the same sign, which is reasonable since $|a_{iso}| \gg |T_{ii}|$. The ambiguity concerning the relative signs can be resolved if the sign of one parameter can be established. In this case a_{iso} is too large to be caused by spin polarization, so that it must be positive (disregarding the sign of the nuclear moment, that is, taking it as positive which is true for ^{13}C). With these assumptions the experimental hyperfine matrixes reported in Table 1 can then be decomposed as given in Equations (3) and (4):

$$\begin{vmatrix} 507.5 & & \\ & 495.2 & \\ & & 629.3 \end{vmatrix} = 544.0 + \begin{vmatrix} -36.5 & & \\ & -48.8 & \\ & & +85.3 \end{vmatrix} \tag{3}$$

$$\begin{vmatrix} 537.5 & & \\ & 518.9 & \\ & & 655.9 \end{vmatrix} = 570.8 + \begin{vmatrix} -33.3 & & \\ & -51.9 & \\ & & +85.1 \end{vmatrix} \tag{4}$$

The large isotropic component is due to unpaired electron spin density in the carbon 2s orbital. The usual interpretation of a_{iso} is then that when divided by the $^{13C}a_{iso}$ atomic value ($^{C}a_0 = 3777$ MHz), it gives an estimate of the contribution of the carbon 2s orbital to the molecular orbital where the unpaired electron is confined. In this way, the carbon 2s character can be estimated to be $c^2_{C2s}(a) = 544/3777 = 0.144$

and $c^2_{C2s}(b) = 570.8/3777 = 0.151$ for species a and b, respectively. The anisotropic part $\boldsymbol{T}$ is nearly cylindrical about the z axis, and originates mainly from spin density in the carbon $2p_z$ orbital. The departure from cylindrical symmetry can be understood considering that a fraction of the spin density is allocated in a 2p orbital perpendicular to the molecular plane, that is, along the x axis in Figure 1. In this way, the $\boldsymbol{T}$-(^{13}C) matrix can be decomposed into two symmetrical tensors oriented along the z and x axis. In the case of species a, this leads to expression (5):

$$\begin{vmatrix} -36.5 & & \\ & -48.8 & \\ & & +85.3 \end{vmatrix} = \begin{vmatrix} -44.7 & & \\ & -44.7 & \\ & & +89.4 \end{vmatrix} + \begin{vmatrix} +8.2 & & \\ & -4.1 & \\ & & -4.1 \end{vmatrix} \quad (5)$$

and, $|-45.7\ -45.7\ +91.4|$ and $|12.4\ -6.2\ -6.2|$, for species b, where the second tensor accounts for the 2p electron population along the x axis owing to the mixing in the $2b_1$ molecular orbital in Walsh's scheme. The resonance data for the $^{13}CO_2^-$ radical may then be interpreted generally in terms of the unpaired electron confined in a carbon sp^2 hybrid orbital ($4a_1$) built up by carbon 2s and $2p_z$ and oxygen $2p_z$ atomic orbitals. The $2p_z$ character of the $4a_1$ molecular orbital can be estimated by comparison with the integral [Eq (6)]:

$$T_0 = 4/5\, g_e\beta_e g_I\beta_n < 1/r^3 >_{np} \quad (6)$$

which is the explicit expression of the dipolar interaction for the external field aligned along the symmetry axis of the $2p_z$ orbital. By adopting $< r^{-3} >_{2p} = 5.820$ a.u.$^{-3}$, $c^2_{C2p_z}$ (a) $= 0.42$ and $c^2_{C2p_z}(b) = 0.43$. Similarly the carbon $2p_x$ character can be determined to be $c^2_{C2p_x}(a) = 0.038$ and $c^2_{C2p_x}(b) = 0.058$ for species a and b, respectively. The total amount of electron spin density accounted for is therefore $\rho^{^{13}C} = 0.60$ and $\rho^{^{13}C} = 0.64$ for species a and b, respectively, leaving the remaining spin density to be shared by the remaining atoms involved in the system (oxygen atoms and surface).

From the relative s and p character on the carbon atom, the O-C-O angle can be determined by assuming that CO_2^- is a trigonal-planar molecule. For a hybridization ratio $\lambda = c_{C2s}/c_{C2p}$, the bond angle α is given by Equation (7):

$$\alpha = 2\cos^{-1}(\lambda^2 + 2)^{-1/2} \quad (7)$$

Substituting the values reported above gives $\alpha \approx 126°$ for both species. It should be noted that the O-C-O angle estimated for the surface-bound radical is smaller than the one obtained with the same method for the same species trapped in solid matrix,[14] and similar to the one observed for Li^+ CO_2^- ion pairs in inert gas matrices.[17]

The 17-oxygen coupling: To obtain information on the spin density distribution over the entire molecule as well as details on the geometry of adsorption, we generated the CO_2^- radical using ^{17}O-enriched CO_2. The spectrum, recorded at 77 K is reported in Figure 4. At high receiver gain, a complex spectral pattern is observed which can be attributed to

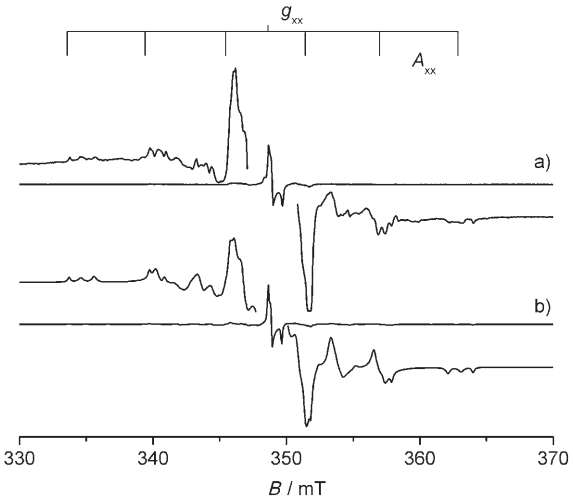

Figure 4. Experimental (a) and simulated (b) EPR spectra of $C^{17}O_2^-$. For the sake of clarity only the A_{xx} component of species a is shown by the stick diagram.

two nearly equivalent ^{17}O nuclei. Since ^{17}O has a nuclear spin 5/2 for each of the principal directions of the $\boldsymbol{g}$ matrix, the signal is additionally split into $2I+1 = 6$ lines in the case of the $C^{17}O^{16}O^-$ isotopomer or into $2nI+1 = 11$ lines for the $C^{17}O^{17}O^-$ species in the case of magnetically equivalent oxygen atoms. On the other hand, in the case of two magnetically non-equivalent nuclei a 36-line pattern is expected for each principal direction of the $\boldsymbol{g}$ tensor. A classic example of the determination of the adsorption structure using an ^{17}O-labeled species is that of the O_2^- radical ion adsorbed on MgO,[31,32] where it displays a side-on structure with magnetically equivalent nuclei, and the same radical adsorbed on Mo/SiO_2,[33] where a top-down structure leads to distinct nonequivalent nuclei. Analysis of the complex spectral pattern reported in Figure 4a was carried out by means of computer simulation. In the simulation we neglected the quadrupole effect ($H_{NQ} = \boldsymbol{IPI}$), which should be added to the spin-Hamiltonian [Eq. (1)] when dealing with nuclei with $I \geq 1$, as in the case of ^{17}O, this term does not influence the powder pattern to an appreciable extent.[31]

The simulation (Figure 4b) was carried out by adding the signals of the three different isotopomers $(C\text{-}^{16}O\text{-}^{16}O)^-$, $(C\text{-}^{17}O\text{-}^{16}O)^-$, and $(C\text{-}^{17}O\text{-}^{17}O)^-$ using the same $\boldsymbol{g}$ and $\boldsymbol{A}$ tensors but weighted by their relative abundance in the gas mixture (see Experimental Section). The contribution of these species to the overall spectrum depends of course on the level of isotopic enrichment. In our case the spectrum is dominated by the $(C\text{-}^{17}O\text{-}^{16}O)^-$ isotopomer. Beside the presence of the different isotopomers, the main source of complexity in the analysis of the spectrum reported in Figure 4 is the presence of multiple species with slightly different

spin-Hamiltonian parameters. This phenomenon, which is a consequence of the heterogeneity of the surface, was already evident in the case of the $^{13}CO_2^-$ spectrum where two species are clearly resolved, while a third one is buried within the spectral envelope. The best fit of the experimental spectrum was obtained by introducing three different species characterized by slightly different hyperfine couplings to the ^{17}O nucleus. The result of the simulation is shown in Figure 4b, while the corresponding spin Hamiltonian parameters are listed in Table 1. It should be emphasized at this stage that the principal axes of the ^{17}O hyperfine tensor may not coincide with the $\boldsymbol{g}$ tensor axes. In the case of ^{17}O-labeled nitrogen dioxide (isoelectronic with CO_2^-) trapped in a single crystal of sodium nitrite,[34] the direction of the two principal components of the dipolar oxygen tensors were actually found to be tilted at 7.5° with respect to the C_{2v} symmetry axis (z axis). However, attempts to simulate the spectrum in Figure 4 by assuming monoclinic symmetry did not lead to any significant improvement in the simulation.

The key to the problem of the surface adsorption geometry is to ascertain the magnetic equivalence of the two oxygen atoms. In the case of two magnetically equivalent nuclei, 11 hyperfine lines are expected for each $\boldsymbol{g}$ principal component. Indication for the presence of these lines can then be found in the outer wings of the spectrum, outside the most congested spectral region, where, however, the line intensity is very low. A magnification of this region is obtained by over amplification of the spectrum, and is shown in Figure 5.

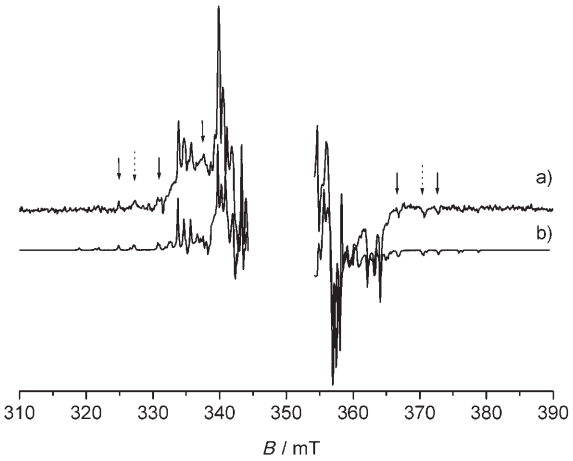

Figure 5. Over amplification of the $C^{17}O^{2-}$ spectrum reported in Figure 4. Only the outer portion of the spectrum is shown. The arrows indicates peaks due to the $2nI+1$ hyperfine structure arising from two magnetically equivalent oxygen atoms. The solid and dotted arrows indicated peaks due to two different species.

A series of weak satellites can actually be observed, which are outlined by the arrows in Figure 5. These lines can be nicely reproduced by the simulation by assuming that the two oxygen nuclei are equivalent (Table 1). The oxygen hyperfine interaction can be analyzed in the usual way by extracting the Fermi contact and dipolar components. Taking the largest of the principal values of $\boldsymbol{A}^O$ to be positive (in the following we associate positive a_{iso} and a positive largest component of $\boldsymbol{T}$ with positive spin density in the s and p orbital, respectively, making the following discussion independent of the signs of the nuclear g factors), the hyperfine tensor can be decomposed in four different ways depending on the sign chosen for the remaining components. Taking the two smallest components with opposite signs leads to asymmetric dipolar tensors and therefore, this option can be discarded. The two remaining options give both two nearly axial dipolar tensors as shown in Equations (8) and (9).

$$\begin{vmatrix} 67.2 & & \\ & 71.5 & \\ & & 169.4 \end{vmatrix} = 102.2 + \begin{vmatrix} -35.0 & & \\ & -30.7 & \\ & & +66.7 \end{vmatrix} \quad (8)$$

$$\begin{vmatrix} -67.2 & & \\ & -71.5 & \\ & & +169.4 \end{vmatrix} = 10.2 + \begin{vmatrix} -77.4 & & \\ & -81.7 & \\ & & +159.2 \end{vmatrix} \quad (9)$$

Departure from axial symmetry can be rationalized in terms of polarization of inner shells and in particular, in analogy with the case of the ^{13}C hyperfine interaction, it can be accounted for by polarization of filled $2p_x$ oxygen orbitals. In this way, the two dipolar tensors can be further decomposed into two axially symmetric contributions along the z and x directions as given in Equations (10) and (11):

$$\begin{vmatrix} -35.0 & & \\ & -30.7 & \\ & & +66.7 \end{vmatrix} = \begin{vmatrix} -32.5 & & \\ & -32.5 & \\ & & +65.0 \end{vmatrix} + \begin{vmatrix} -2.4 & & \\ & +1.7 & \\ & & +1.7 \end{vmatrix} \quad (10)$$

$$\begin{vmatrix} -77.4 & & \\ & -81.7 & \\ & & +159.2 \end{vmatrix} = \begin{vmatrix} -80.3 & & \\ & -80.3 & \\ & & +160.6 \end{vmatrix} + \begin{vmatrix} +2.8 & & \\ & -1.4 & \\ & & -1.4 \end{vmatrix} \quad (11)$$

The first choice, that is, the one in which all matrix components have the same sign, leads to a nearly symmetrical dipolar $\boldsymbol{T}$ tensor whose decomposition [Eq. (10)] gives a value of 65.0 MHz for the principal components along the z direction. From the analysis of the ^{13}C hyperfine interaction a residual spin density $\rho^O = 0.4$ was found to be spread over the oxygen atoms. Assuming that the unpaired electron is confined in the oxygen p_z orbital and considering that the two oxygen atoms are magnetically equivalent, the dipolar component can be estimated to be 67.35 MHz, taking the atomic value for the dipolar ^{17}O hyperfine constant $T_0 = 4/5 g_e \beta_e \, g_O \beta_O \langle r^{-3} \rangle = 336.8$ MHz, which is in good agreement with the experimental value. On the other hand the other choice [Eq. (9)] leads to an exceedingly high value for the dipolar interaction, which is not compatible with the ^{13}C results. Also it should be noted that in the first case, the dipolar tensor components along the z and x directions indicate

that the spin densities are positive in the $2p_z$ orbital but negative in the $2p_x$ orbital in line with the case of the trapped NO_2 radical[34] and for orthogonal $2p_\pi$ orbitals of the superoxide radical anion.[31] Adopting the reported atomic values for the dipolar (${}^{C}T_0 = 214.8$ MHz, ${}^{O}T_0 = 336.8$ MHz) and isotropic (${}^{C}a_0 = 3777$ MHz ${}^{O}a_0 = 5263$ MHz) ^{13}C and ^{17}O hyperfine constants, the total spin density over the CO_2^- radical can then be calculated to be for the main species: $\rho^{tot} = \rho^{C}_{2s} + \rho^{C}_{2p_z} + \rho^{C}_{2p_x} + 2(\rho^{O}_{2s} + \rho^{O}_{2p_z} + \rho^{O}_{2p_x}) = 1.00$, which indicates that within the limits of the approximation adopted, the electron transfer from the surface $(H^+)(e^-)$ centers towards the adsorbed molecule is virtually complete. An analogous treatment applied to the other resolved species leads to the parameters listed in Table 2.

Table 2. Spin densities in the various carbon and oxygen orbitals of the CO_2^- radical derived from experimental spectra.

Species	$\rho^C(2s)$	$\rho^C(2p_z)$	$\rho^C(2p_x)$	$\rho^O(2s)$	$\rho^O(2p_z)$	$\rho^O(2p_x)$	ρ^{tot}
a	0.144	0.416	0.038	0.019	0.193	−0.008	1.00
b	0.151	0.425	0.058	0.020	0.149	−0.006	0.96
c		unresolved		0.019	0.133	−0.006	–

Structural models of the surface-stabilized CO_2^- radical: From these results, and in particular from the ^{17}O hyperfine tensors, important structural information relative to the surface stabilized radical are obtained. The surface CO_2^- species bears, as expected, a bent structure, with a O-C-O angle of about 126° which is in line with what observed in the case of the same species trapped in solid matrixes.[14–17] Most importantly the magnetic equivalence of the two oxygen nuclei also requires structural equivalence, as already observed in the case of other radicals such as N_2^- and O_2^- stabilized on the same surface.[29,31] This poses, together with the known morphology of MgO, and the topographical details of the $(H^+)(e^-)$ centers, which have been recently clarified,[27] some important constraints to the possible adsorption sites for the CO_2^- radical. We recently proposed a general assignment of the $(H^+)(e^-)$ paramagnetic centers formed at the MgO surface, which consists of electron-proton pairs stabilized at low coordinate Mg^{2+}–O^{2-} ions at edges, corners, and reverse corners. We propose then that the CO_2^- radicals formed upon direct electron transfer remain stabilized on the same sites, as in the case of O_2^- formed under the same conditions. Based on these considerations, we can then assign the main species to CO_2^- adsorbed on four and three-coordinate Mg^{2+} ions at MgO edges and corners as schematically shown in Figure 6, while the third species may be ascribed to radicals adsorbed at reverse corner sites. The magnetic equivalence of the oxygen atoms allows us in fact to exclude side-on type structures, while a carbon-down configuration seems to be unlikely based on simple considerations of charge distribution within the molecular fragment. The structure proposed in Figure 6 is then not only compatible with the experimental data but also makes "chemical" sense and reflects the known structure of sodium formate, where C and Na lie on the unique axis of symmetry. This assignment should be confirmed in the future by means of accurate theoretical calculations.

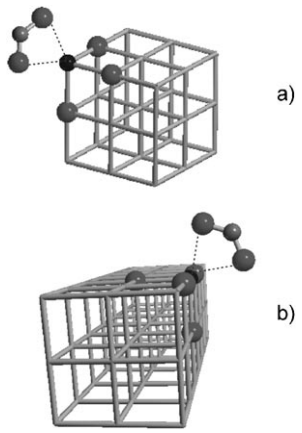

Figure 6. Schematic representation of the adsorbed CO_2^- radical ion at corners (a) and edges (b) of MgO as deduced from the experimental data.

Conclusion

We report herein the first complete EPR characterization of the CO_2^- radical adsorbed on polycrystalline MgO and formed by direct electron transfer from surface $(H^+)(e^-)$ centers. The carboxylate radical anion, which represents the first step in the reductive activation of the CO_2 molecule, has a bent structure with an angle of about 126°. The 17-Oxygen resolved hyperfine structure allowed us to fully determine the spin density distribution within the SOMO orbital and to ascertain the magnetic equivalence of the two oxygen atoms. Based on the experimental data, we propose that the CO_2^- radical ion displays a side-on structure with the two oxygen atoms symmetrically disposed with respect to four- and three-coordinate Mg^{2+} ions.

Experimental Section

High surface area polycrystalline MgO was prepared by slow decomposition of $Mg(OH)_2$ in a vacuum as described in reference [27]. The MgO powder was activated at 1173 K to remove surface-adsorbed impurities. (H+)(e−) centers were generated on the surface of the activated oxide by contacting the solid with H atoms produced in a 2.45 GHz microwave glove discharge under static conditions. Analogous results were obtained by irradiating the solid with UV light under an H_2 atmosphere (10 mbar). UV irradiation of the sample was carried out at 77 K with a 500-W Oriel Instrument UV lamp, incorporating a Hg/Xe arc lamp (250 nm to $>$ 2500 nm), in conjunction with a water filter. In both cases (reaction with H atoms or UV irradiation in H_2) the sample develops a blue coloration, indicating the formation of surface $(H^+)(e^-)$ centers. High purity

$^{13}CO_2$ (90% ^{13}C enrichment) and $C^{17}O_2$ (51% ^{17}O enrichment) were used. All gases were purified with the freeze–thaw–pump method. All isotopically labeled CO_2 products were supplied by Icon Services New Jersey. EPR spectra were recorded at 298 K and 77 K on a Bruker EMX spectrometer operating at X-band frequencies and equipped with a cylindrical cavity operating at a 100-KHz field modulation. The spectra were recorded at 1-mW microwave power. The CW-EPR spectra were simulated by using the EPRsim32 program.[35]

Acknowledgement

This work has been supported by the Italian MIUR through a Cofin 2005 project.

[1] H. Arakawa et al., *Chem. Rev.* **2001**, *101*, 953.
[2] Proceedings of the 7th International Conference on Carbon Dioxide Utilization, *Stud. Surf. Sci. Catal.*, *Vol. 153* (Eds.: S-E. Park, J-S. Chang, K-W. Lee), Seoul, **2004**.
[3] H. Huber, D. McIntosh, G. A. Ozin, *Inorg. Chem.* **1978**, *16*, 975.
[4] G. A. Ozin, H. Huber, D. McIntosh, *Inorg. Chem.* **1978**, *17*, 1472.
[5] D. H. Gibson, *Coord. Chem. Rev.* **1999**, *185–186*, 335.
[6] H.-J. Freund, M. W. Roberts, *Surf. Sci. Rep.* **1996**, *25*, 225.
[7] M. Ramin, J.-D. Grunwaldt, A. Baiker, *J. Catal.* **2005**, *234*, 256.
[8] K. Yamaguchi, K. Ebitani, T. Yhoshida, H. Yoshida, K. Kaneda, *J. Am. Chem. Soc.* **1999**, *121*.
[9] M. Tu, R. J. Davis, *J. Catal.* **2001**, *199*, 85.
[10] R. N. Compton, P. W. Reinhardt, C. D. Cooper, *J. Chem. Phys.* **1975**, *63*, 3821.
[11] A. D. Walsh, *J. Chem. Soc.* **1953**, 2266.
[12] M. E. Jacox, W. E. Thompson, *J. Chem. Phys.* **1989**, *91*, 1410.
[13] D. W. Ovenall, D. H. Whiffen, *Proc. Chem. Soc.* **1960**, 420.
[14] D. W. Ovenall, D. H. Whiffen, *Mol. Phys.* **1961**, *4*, 135.
[15] B. Mile, *Angew. Chem.* **1968**, *80*, 519; *Angew. Chem. Int. Ed. Engl.* **1968**, *7*, 507.
[16] J. E. Bennett, S. C. Graham, B. Mile, *Spectrochim. Acta Part A* **1973**, *29*, 375.
[17] Z. H. Kafafi, R. H. Hauge, W. E. Billups, J. L. Margrave, *J. Am. Chem. Soc.* **1983**, *105*, 3886.
[18] F. Solymosi, *J. Mol. Catal.* **1991**, *65*, 337.
[19] O. Seiferth, K. Wolter, H. Kuhlenbeck, H.-J. Freund, *Surf. Sci.* **2002**, *505*, 215.
[20] T. Inoue, A. Fujishima, S. Konishi, K. Honda, *Nature* **1979**, *277*, 637.
[21] K. R. Thampi, J. Kiwi, M. Gratzel, *Nature* **1987**, *327*, 506.
[22] K. Ikeue, H. Yamashita, M. Anpo, T. Takewaki, *J. Phys. Chem. B* **2001**, *105*, 8350.
[23] J. S. Hwang, J. S. Chang, S. E. Park, K. Ikeue, M. Anpo, *Top. Catal.* **2005**, *35*, 311.
[24] F. Saladin, I. Alxneit, *J. Chem. Soc. Faraday Trans.* **1997**, 4159.
[25] K. Teramura, T. Tanaka, H. Ishikawa, Y. Kohono, T. Funabiki, *J. Phys. Chem. B* **2004**, *108*, 346.
[26] J. H. Lunsford, J. P. Jayne, *J. Phys. Chem.* **1965**, *69*, 2182.
[27] M. Chiesa, M. C. Paganini, G. Spoto, E. Giamello, C. Di Valentin, A. Del Vitto, G. Pacchioni, *J. Phys. Chem. B* **2005**, *109*, 7314.
[28] M. Chiesa, M. C. Paganini, E. Giamello, C. Di Valentin, G. Pacchioni, *ChemPhysChem* **2006**, *7*, 728.
[29] M. Chiesa, E. Giamello, D. Murphy, G. Pacchioni, M. C. Paganini, R. Soave, Z. Sojka, *J. Phys. Chem. B* **2001**, *104*, 497.
[30] A. Carrington, A. D. McLachlan, *Introduction to Magnetic Resonance*, Harper & Row, New York, **1967**, p. 138.
[31] M. Chiesa, E. Giamello, M. C. Paganini, Z. Sojka, D. M. Murphy, *J. Chem. Phys.* **2002**, *116*, 4266.
[32] M. Che, A. J. Tench, *Adv. Catal.* **1982**, *31*, 77.
[33] M. Che, E. Giamello, A. J. Tench, *Colloids Surf.* **1985**, *13*, 231.
[34] Z. Luz, A. Reuveni, R. W. Holmberg, B. L. Silver *J. Chem. Phys.* **1969**, *51*, 4017.
[35] A. Adamski, T. Spalek, Z. Sojka, *Res. Chem. Intermed.* **2003**, *29*, 793.

Received: June 6, 2006
Published online: December 6, 2006

